JACS
JOURNAL OF THE AMERICAN CHEMICAL SOCIETY
pubs.acs.org/JACS
Article

Radical Isomerization upon Dissociative Electron Ionization of Anthracene and Phenanthrene

Madison M. Patch, Rory McClish, Sanjana Panchagnula, Daniël B. Rap, Shreyak Banhatti, Helgi R. Hrodmarsson, Sandra Brünken, Harold Linnartz, Alexander G. G. M. Tielens, and Jordy Bouwman*

Cite This: J. Am. Chem. Soc. 2025, 147, 34508−34516
Read Online
ACCESS | Metrics & More | Article Recommendations | Supporting Information

ABSTRACT: Polycyclic aromatic hydrocarbons (PAHs) are abundantly present in space. The grandPAH hypothesis states that small PAHs are photodissociated, while large symmetric PAHs survive the harsh environments in space. Moreover, it has been hypothesized that large aromatic molecules (C_nH_m with $n \geq 60$) can convert to buckminsterfullerene (C_{60}). In this work, we test these hypotheses by studying the products formed upon dissociative electron ionization of two isomeric $C_{14}H_{10}$ PAHs, anthracene and phenanthrene. The fragment ions that are formed following H loss and H_2 loss are isolated in a cryogenically-cooled 22-pole ion trap and tagged with neon. Infrared predissociation spectra are recorded of the thus formed van der Waals bound complexes and the PAH dissociation fragments are identified based on a comparison with density functional theory (DFT) calculated spectra. The ionized PAHs undergo radical isomerization prior to the loss of H or H_2, resulting in a highly symmetric daughter ion that is identical for the two distinctly different parent PAHs. Moreover, the product ions are found to obey the isolated pentagon rule, which also curves fullerenes and contributes to their structural stability. We propose a mechanism for the radical isomerization based on existing molecular dynamics simulations from the literature augmented by DFT calculations. This study lends credit to the grandPAH hypothesis by showing that PAH species isomerize drastically to form a new molecule that is highly symmetric. Moreover, the formation of a daughter species that obeys the isolated-pentagon rule suggests that there is a strong chemical link between interstellar PAHs and fullerenes.

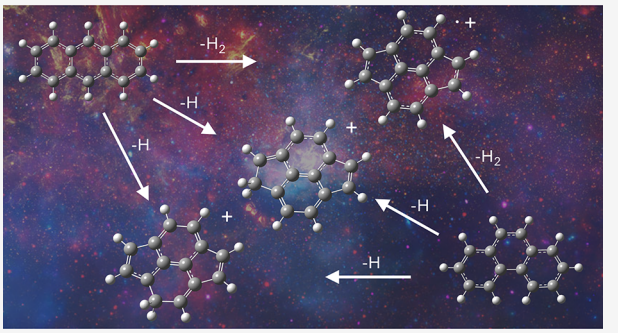

1. INTRODUCTION

Polycyclic aromatic hydrocarbons (PAHs) are found in a large variety of interstellar environments, ranging from HII regions, reflection nebulae, young stellar objects (YSOs), planetary nebulae, to post-asymptotic giant branch (AGB) stars.[1−3] They are identified based on the characteristic mid-infrared (mid-IR) emission features that they emit after being excited by strong ultraviolet (UV) radiation from nearby stars.[4−6] It has been estimated that up to 20% of the total cosmic carbon budget is locked-up in PAHs, making them key species in the cosmic carbon cycle.[2] For a long time, PAHs were only detected as a class of molecules carrying the mid-IR vibrational bands from UV bright sources, but unambiguous identifications of PAHs and cyano-substituted PAHs have recently been made through their pure rotational transitions in radio astronomical surveys of cold dark molecular cloud cores.[7−10]

While the initial consensus in the field was that the interstellar PAH family is very diverse, more recent observations reveal that, likely, only a few, large, and compact "grandPAHs" dominate the PAH population in photon dominated regions.[11,12] Specifically, the IR emission spectra observed toward the brightest emission zones in galactic and extragalactic objects are strikingly similar.[13] While PAHs, as a class, have very similar intrinsic spectra dominated by CH and CC stretching and bending modes, individual spectra show subtle spectral variations in peak position.[14−16] These two aspects, astronomical and molecular spectroscopy, can be reconciled if just a few PAHs dominate the interstellar PAH family: the so-called grandPAHs. Extensive studies of the spectroscopic properties of PAHs have not been able to uniquely identify grandPAHs. Such studies[14,16] have generally focused on the thermodynamically most stable PAHs in the highly condensed and symmetric pyrene, coronene, and ovalene families.[6,17]

Thermodynamics considerations play an important role in the formation of PAHs in sooting flames, but in general, kinetics dominate interstellar chemistry. Specifically, in photo-

Received: May 21, 2025
Revised: August 27, 2025
Accepted: August 28, 2025
Published: September 12, 2025

https://doi.org/10.1021/jacs.5c08619
J. Am. Chem. Soc. 2025, 147, 34508−34516

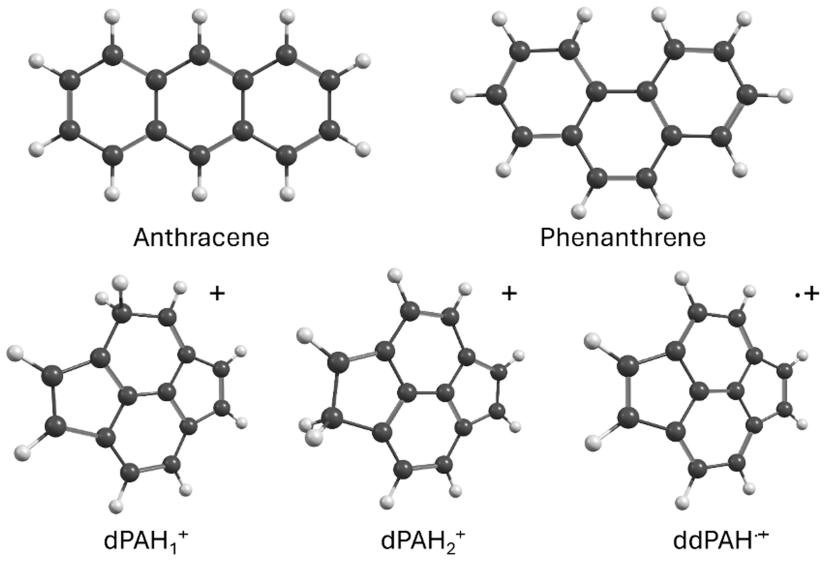

Figure 1. Structures of the two isomeric $C_{14}H_{10}$ parent compounds, anthracene (top left) and phenanthrene (top right), used in this study. Using infrared predissociation spectroscopy, we identify the structures **dPAH$_1^+$** and **dPAH$_2^+$** as the products formed via single dehydrogenation of the parent ion. The **ddPAH$^{\bullet+}$** species—known as pyracyclene—is formed through double dehydrogenation of the parent ion.

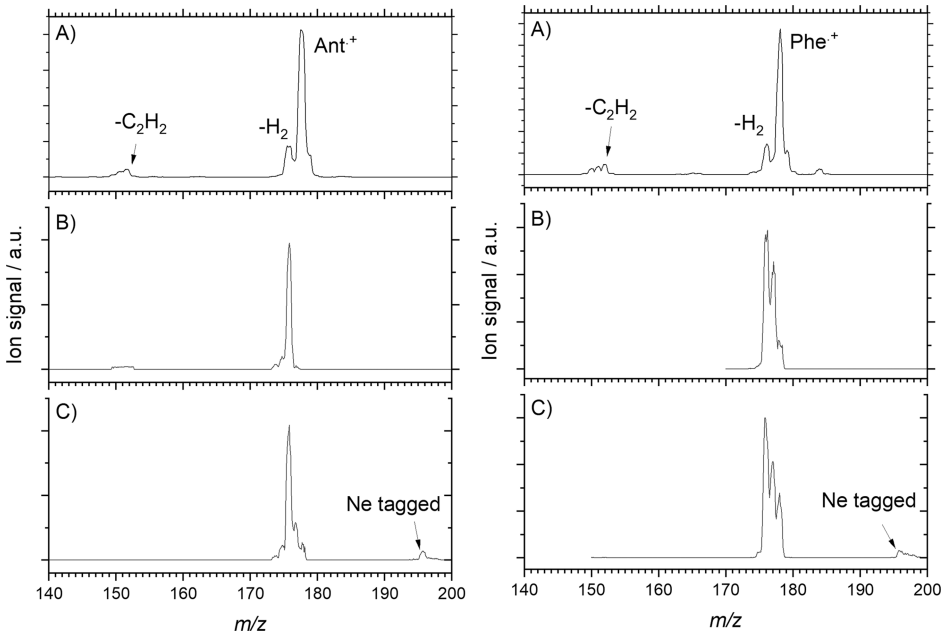

Figure 2. (A) Electron ionization mass spectra of anthracene (left) and phenanthrene (right) recorded at an electron energy of 30 eV, (B) mass spectrum of the mass-selected ions admitted to the cryogenic ion trap, and (C) mass spectrum of the contents of the trap after tagging the ions with neon.

dissociation regions (PDRs), the prevalent, strong far-ultraviolet photon field opens up new chemical pathways, driving the composition away from thermodynamically favored species. First, only large PAHs consisting of more than $\gtrsim$30 carbon atoms can survive, while smaller irregular species undergo photochemical C_2H_2 loss.[18−21] Experiencing multiphoton excitations, larger, more symmetric PAHs are first fully stripped from all their H atoms before the carbon skeleton starts to shrink through C_2 loss.[22,23] In the process, the carbon backbone likely isomerizes, and it has been hypothesized that interstellar C_{60} buckminsterfullerene results from photodissociation and photoisomerization of large interstellar PAHs ($N_C \geq 60$).[20] A laboratory study has indeed suggested that a stable C_{60}^+ species forms upon the dissociation of a large cationic PAH.[23] A firm spectroscopic identification of the buckminsterfullerene radical cation formed by this process has not yet been made. Moreover, very little is known about the species that form upon photoinduced isomerization of interstellar PAHs, but these species may be key carriers of the IR emission bands.

Various physicochemical tools in combination with quantum chemical calculations have been employed to study the dissociation mechanisms of smaller PAHs and their cations.[21,22,24−30] A few studies that focused on revealing the molecular structure of the dissociation fragment ions formed upon losing C_2H_2 and HCN from PAHs and heterocyclic

https://doi.org/10.1021/jacs.5c08619
J. Am. Chem. Soc. 2025, 147, 34508−34516

PAHs, respectively, have found that five-membered rings are included upon multiphoton dissociative ionization or electron ionization.[24,31,32] A particularly interesting process from an interstellar perspective is the dehydrogenation of PAHs, which is thought to play a critical role in the formation of interstellar hydrogen.[33−35] Previous studies on PAH dissociation mechanisms revealed that this process begins with the loss of hydrogen atoms.[22,30,35] The structures of the small monodehydrogenated PAH cations naphthyl, phenanthryl, and pyrenyl generated by 193 nm multiphoton dissociative ionization of their halogenated parent PAHs have been studied by means of infrared multiphoton dissociation (IRMPD) spectroscopy, resulting in broad absorption bands that are difficult to uniquely assign.[36,37] A recent study on the double dehydrogenation of the pyrene cation using infrared predissociation (IRPD) spectroscopy—which gives rise to better resolved spectra than IRMPD—showed that such a small pericondensed PAH tends to lose hydrogen atoms from adjacent carbon atoms on the periphery (4,5 or 1,2 position), or from the 1,3 position, without altering the backbone of carbon atoms.[38]

Here, we identify the product ions that form from 30 eV electron-induced dissociative ionization of two $C_{14}H_{10}$ isomers, anthracene and phenanthrene (Figure 1), to simulate the effect of energetic processing of prototypical catacondensed PAHs in the interstellar medium (ISM). The daughter ions formed by the loss of H or H_2 (or 2H) are isolated in a cryogenically cooled 22-pole ion trap, and the IRPD spectra of the neon-tagged daughter ions are recorded. The structures of the daughter ion species are assigned by comparing the experimental spectra to density functional theory (DFT) calculated spectra. Next, potential energy surface (PES) calculations are presented that help rationalize the formation of the detected product species. Finally, the findings are considered in an astrochemical context, leading to conclusions on the photoisomerization of PAHs and the probable contributors to interstellar aromatic IR emission bands.

2. RESULTS AND DISCUSSION

Experiments were conducted on the cryogenically cooled 22-pole ion trap instrument FELion connected to the free electron laser for infrared experiments (FELIX).[58] The dissociation product of interest was isolated in the trap and tagged with a weakly bound neon atom, and the predissociation spectrum was recorded. Further experimental details are provided in the Experimental Section.

2.1. Mass Spectrometry. The electron ionization mass spectra for anthracene and phenanthrene were recorded at an electron energy of 30 eV and are shown in Figure 2A. From these spectra, it can be seen that the radical cation of the parent species is accompanied by the product formed through single dehydrogenation (m/z 177), double dehydrogenation (m/z 176), as well as the loss of C_2H_2 (m/z 152).

Next, only a mass band corresponding to the product ions of interest, i.e., **dPAH**$^+$ and **ddPAH**$^{\bullet+}$, were admitted to the ion trap by selecting their m/z using the quadrupole mass filter in front of the entrance to the 22-pole trap. The mass filter is somewhat broad, resulting in a range of masses being admitted to the cryogenically cooled trap (Figure 2 panel B). In the trap, these mass-selected ions were subsequently exposed to a short pulse of a rare gas mixture (He/Ne in a 3:1 ratio) to cool the ions and to generate the ion−Ne complex. This resulted in weakly bound complexes at m/z 197 and 196 for the mono- and doubly dehydrogenated anthracene and phenanthrene cations, respectively (Figure 2, panel C). These tagged complex signals were monitored after selection with a second quadrupole mass filter as a function of frequency to construct the IRPD spectra.

2.2. Infrared Predissociation Spectroscopy. *2.2.1. Doubly Dehydrogenated* ***Ant***$^{\bullet+}$ *and* ***Phe***$^{\bullet+}$. The infrared predissociation spectra of doubly dehydrogenated anthracene (**ddAnt**$^{\bullet+}$) and phenanthrene (**ddPhe**$^{\bullet+}$) are shown in light blue and dark blue, respectively, in Figure 3. The experimental spectra are normalized to the strongest absorption in the measured wavelength region, which occurs at ∼1300 cm^{-1}. At first glance, the mid-IR spectra of **ddAnt**$^{\bullet+}$ and **ddPhe**$^{\bullet+}$ are identical, and only very subtle differences appear to be present, if any. This is an interesting observation, as the molecular structures of the parent species, anthracene and phenanthrene, are very different, and the spectra of the cation (and dication) of these species reveal that no significant isomerization is apparent for the parent species.[32] Moreover, there is no obvious connection between the two dehydrogenation products of these two distinct isomers. Another noteworthy observation is that there are only a few infrared-active modes for this molecule of $C_{14}H_8^{\bullet+}$ composition, which hints at a species that is likely of high symmetry.

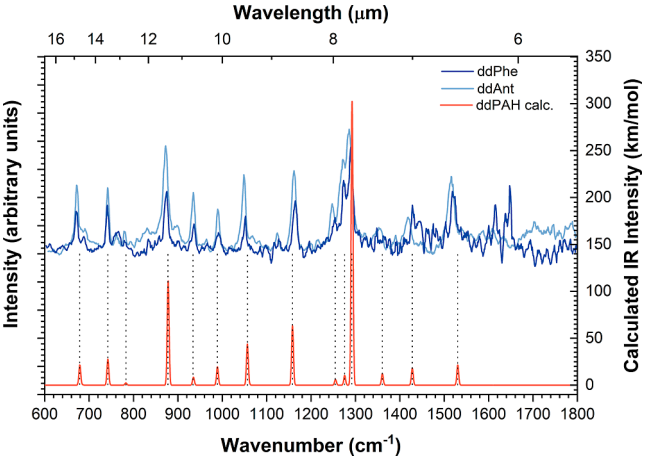

Figure 3. IRPD spectra of the doubly dehydrogenated anthracene (light blue) and doubly dehydrogenated phenanthrene (dark blue) cations. Shown in red is the computed spectrum of the **ddPAH**$^{\bullet+}$ species (structures in Figure 1). The computed spectrum is calculated using B3LYP/6-311++G(2d,p), and the frequencies have been scaled using a factor of 0.983 to account for anharmonicities. The resulting stick spectrum is convolved with a Gaussian function with a width of 5 cm^{-1} to facilitate comparison with the experimental data.

Also shown in Figure 3 is the harmonic spectrum of the **ddPAH**$^{\bullet+}$ species pyracyclene (structure in Figure 1) calculated using the B3LYP/6-311++G(2d,p) functional and basis set and scaled to account for anharmonicities. For ease of comparison, the computed spectrum has been convolved with a Gaussian shape with an FWHM of 5 cm^{-1} that corresponds to the experimental resolution. A comparison between the measured and calculated band positions is shown in Table S1 in the Supporting Information. Among the many isomers we examined, the **ddPAH**$^{\bullet+}$ species pyracyclene emerged as the most energetically stable, being more than 42 kcal/mol lower in energy than all others. None of the direct dehydrogenation products of anthracene or phenanthrene yield a match (Figures

https://doi.org/10.1021/jacs.5c08619
J. Am. Chem. Soc. 2025, 147, 34508−34516

S1−S12 in the Supporting Information). However, the computed spectrum of pyracyclene is well-matched with the band positions of the experimental spectrum. The average absolute deviation from the calculated band positions is 5 cm^{-1}. Some mismatches are apparent that can be caused by overtones and resonances that are not captured in the harmonic calculations. Moreover, small spectral shifts might be induced by attaching a neon tag to the daughter ion. Lastly, the bands that are seen beyond 1600 cm^{-1} in the **ddPhe**$^{\bullet+}$ data are likely artifacts.

Saturation-depletion scans were conducted on both **ddAnt**$^{\bullet+}$ and **ddPhe**$^{\bullet+}$ to estimate what fraction of ions in the trap is in the form of the assigned species. To this end, we set the laser to the central positions where strong absorption bands are observed and recorded the depletion of the tagged ion signal as a function of time. The leftover fraction of ions gives an upper limit on the total contribution of other isomers to the signal. An IR spectrum with depletion values for the various bands in the **ddAnt**$^{\bullet+}$ and **ddPhe**$^{\bullet+}$ spectra is shown in Figure S13 in the Supporting Information. From these depletion data, we estimate that at most 20% is in the form of isomers other than the pyracyclene ion shown in Figure 1.

2.2.2. Singly Dehydrogenated ***Ant***$^{\bullet+}$ *and* ***Phe***$^{\bullet+}$. The spectra of the singly dehydrogenated Ant and Phe species (**dAnt**$^{+}$ and **dPhe**$^{+}$) were recorded and are shown in Figures 4

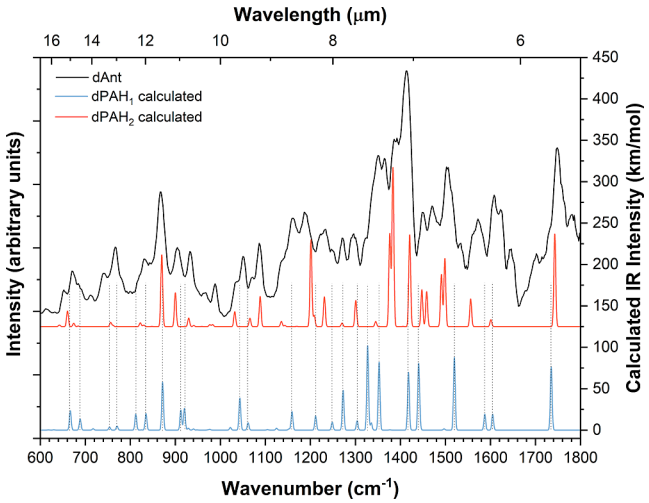

Figure 4. Black trace represents the experimental spectrum for singly dehydrogenated anthracene. The blue and red traces represent the spectra of singlet **dPAH**$_1^+$ and **dPAH**$_2^+$ (offset by 125 km/mol) computed at the B3LYP/6-311++G(2d,p) level of theory and scaled using a factor of 0.983. The molecular structures for **dPAH**$_1^+$ and **dPAH**$_2^+$ are shown in Figure 1.

and 5. In these figures, the experimental traces are shown in black, and the calculated spectra of the singlets states of **dPAH**$_1^+$ and **dPAH**$_2^+$ (see Figure 1 for their molecular structures) are added in blue and red, respectively. Based on DFT calculations, the triplet states were found to be higher in energy than the singlets by 9 and 18 kcal/mol for **dPAH**$_1^+$ and **dPAH**$_2^+$, respectively, and were found to not provide a good match with the experimental IR spectrum. From Figures 4 and 5, it can be seen that more modes are IR-active in the experimental spectrum compared to the **ddPAH**$^{\bullet+}$ spectrum, suggesting contributions of multiple isomers and/or reduced symmetry of the daughter ion. Similar to the case for **ddPAH**$^{\bullet+}$, the two experimental spectra are very similar but

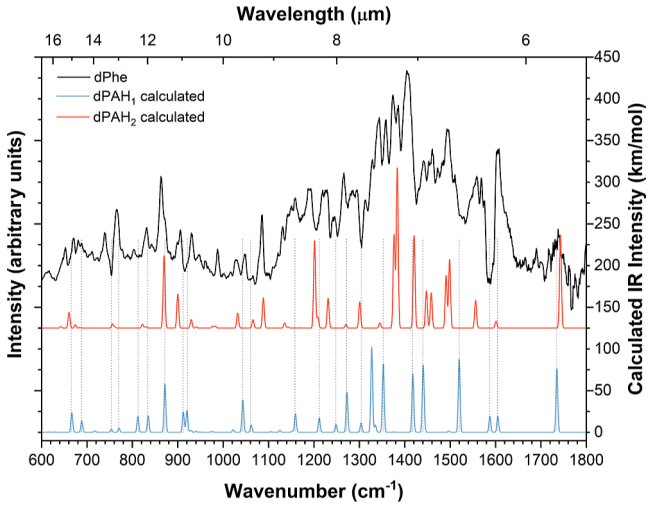

Figure 5. Black trace represents the experimental spectrum for singly dehydrogenated phenanthrene. The blue and red traces represent the spectra of singlet **dPAH**$_1^+$ and **dPAH**$_2^+$ (offset by 125 km/mol) computed at the B3LYP/6-311++G(2d,p) level of theory and scaled using a factor of 0.983. The molecular structures for **dPAH**$_1^+$ and **dPAH**$_2^+$ are shown in Figure 1.

with a notable difference in the improved signal-to-noise ratio in the **dAnt**$^{+}$ spectrum.

A comparison between the experimentally measured band positions and the computed (scaled) harmonic modes is shown in Tables S2 and S3 in the Supporting Information. The band positions of the computed spectrum align well with the measured data, with an average absolute deviation of 7 cm^{-1} and 3 cm^{-1} for the **dAnt**$^{+}$ and **dPhe**$^{+}$ data, respectively, and a maximum deviation of 12 cm^{-1}. Moreover, the experimental spectrum is well-represented by the combination of both isomers. Saturation-depletion scans for the singly dehydrogenated phenanthrene species are shown in Figure S14. These data are consistent with two isomers contributing to the spectrum in approximately equal amounts.

2.3. PES Calculations. PES calculations were performed to yield insights into the possible formation mechanism of the identified isomers, and the resulting PES is shown in Figure 6. We do not attempt to provide a full PES but rather only explore viable pathways to the observed products starting from reaction intermediates that were previously identified in the literature.

In Figure 6, we start from **Int1** as this was identified as an intermediate for the loss of C_2H_2 from **Ant**$^{\bullet+}$ using molecular dynamics (MD) simulations.[32] We note here that these pathways all involve hydrogen migration and isomerization of internally excited **Ant**$^{\bullet+}$ and **Phe**$^{\bullet+}$ before the loss of H or H_2. This was also the dominant order seen in Banhatti et al.[32] for the loss of C_2H_2. Isomerization after the loss of H or H_2 cannot be entirely excluded but is less likely since the dissociation requires substantial energy that is no longer available in the system to overcome isomerization barriers. MD calculations on the dissociation of other energized PAH cations have shown that in general, isomerization precedes dissociation.[39]

Int1 is found to connect to **Int2**, which was also located on the **Phe**$^{\bullet+}$ PES by MD simulations.[32] We find that the two intermediates are connected via a series of hydrogen migrations (Figure S15 in the Supporting Information) that have a rate-limiting transition state (**TS1**) located at 57 kcal/mol relative to **Int2**. A hydrogen transfer from **Int2** over **TS2**

https://doi.org/10.1021/jacs.5c08619
J. Am. Chem. Soc. 2025, 147, 34508−34516

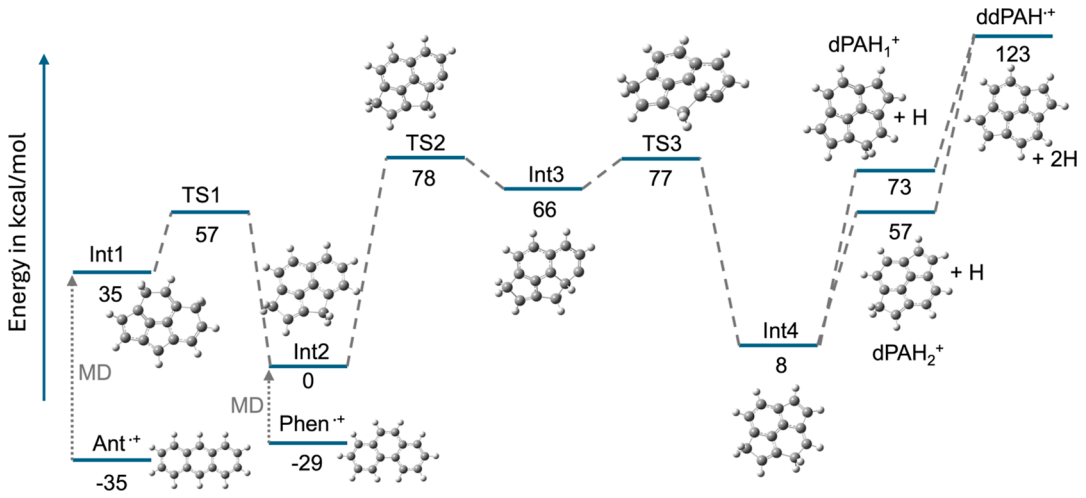

Figure 6. A $C_{14}H_{10}^{\bullet+}$ PES calculated using B3LYP/6-311++G(2d,p) showing a reaction mechanism that connects intermediate structures that were found using MD simulations (**Int1** and **Int2**, see Banhatti et al.[32]) with the products that are identified in this work ($\mathbf{dPAH_1}^+$, $\mathbf{dPAH_2}^+$, and $\mathbf{ddPAH}^{\bullet+}$). The transition state connecting **Int1** and **Int2** displays only the rate-limiting step (**TS1**), but the full surface is available from the Supporting Information.

at 78 kcal/mol results in **Int3** at 66 kcal/mol. **Int3** undergoes a 5−6 to 6−5-membered ring isomerization over **TS3** at 77 kcal/mol, which results in the isolation of the two five-membered rings in the resulting **Int4** at 8 kcal/mol. From here, hydrogen loss can yield either $\mathbf{dPAH_1}^+$ at 73 kcal/mol or $\mathbf{dPAH_2}^+$ at 57 kcal/mol. Alternatively, **Int4** can lose both hydrogen atoms to form $\mathbf{ddPAH}^{\bullet+}$ at 123 kcal/mol.

The ionization energies are 7.439 and 7.891 eV for anthracene and phenanthrene, respectively.[40] The activation energies for H loss from anthracene cation, followed by a subsequent H loss from the resulting $C_{14}H_9^{\bullet+}$, were calculated to be 4.28 and 2.71 eV (99 and 62 kcal/mol), respectively.[25] Consequently, the appearance energies for removing one and two hydrogen atoms from neutral anthracene are 270 and 333 kcal/mol, respectively. In our experiment, the maximum energy imparted to the parent ion after electron ionization at 30 eV is 520 kcal/mol for anthracene and 510 kcal/mol for phenanthrene. Therefore, while the barrier heights of all of the transition states involved in the transformation of $\mathbf{Ant}^{\bullet+}$ and $\mathbf{Phe}^{\bullet+}$ to **Int1** and **Int2** remain unknown, the available energy in our system is more than sufficient to facilitate isomerization to the observed products.

3. IMPLICATIONS AND CONCLUSIONS

The $C_{14}H_9^+$ and $C_{14}H_8^{\bullet+}$ species that form upon dissociative ionization of anthracene and phenanthrene have been identified by means of cryogenic ion IR predissociation spectroscopy. A surprising radical isomerization of the parent ion is found to precede the loss of H and H_2. The identified products are the most energetically favorable species for their specific chemical composition and obey the isolated pentagon rule.[41−43] The product ions identified in this work have their five-membered-ring structures on the periphery of the molecule. When extrapolating to larger molecules, similar isomerizations involving H-migration and H-loss processes can be expected upon energetic processing, be it thermally by electrons, photons, or cosmic rays. In large PAHs, the defects may initially form at the periphery of the parent ion, but they are expected to migrate inward[44,45] via 6−5 to 5−6-membered-ring isomerizations and could curl the molecular framework. We emphasize that if this type of isomerization occurs in large, irregular aromatic molecules in the ISM, fullerenes are highly likely to form from interstellar PAHs.

The grandPAH hypothesis suggests that small PAHs get photodissociated and only large PAHs survive in the ISM. Earlier studies have shown that PAHs of astronomically relevant sizes dehydrogenate when they are energetically processed by irradiation, which could play a role in the formation of interstellar hydrogen.[33−35] However, the process of isomerization preceding the dehydrogenation of PAHs in the ISM has been completely overlooked. The interstellar PAHs that have historically been considered are similar to those that are formed through thermodynamically driven processes, as seen in flames. In this work, we show that radical isomerization takes place even before the first (one or two) hydrogen atoms are lost. This implies that PAHs in PDRs, PNes, RNes, and YSOs in the ISM must undergo similar structural changes, driving the interstellar PAH population away from historically considered PAHs. We show that energetic processing results in a set of highly symmetric and compact PAHs that include both five- and six-membered ring structures. Due to their high symmetry and compactness, PAHs formed through these isomerization routes fulfill the observational constraints for the carriers of the interstellar IR emission bands. Species such as $\mathbf{ddPAH}^{\bullet+}$ and similar larger molecular species, as well as their neutral counterparts that may form through neutralization via collision with an electron, need to be included in the NASA Ames PAH database to enable the analysis of IR emission bands.[46] Moreover, the identification of the $dPAH^+$ isomers in space will be aided by their nonzero dipole moment, which will make their pure rotational spectra suitable for systematic surveys.

The symmetric and highly stable molecules that form through the photoprocessing and photoisomerization of PAHs also need to be considered as potential carriers of diffuse interstellar bands (DIBs). DIBs comprise over 500 absorption bands that have been detected throughout the UV, optical, and IR regions of the electromagnetic spectrum and whose carriers have (largely) remained a mystery for over a century.[47] Only very recently, electronic transitions of C_{60}^+ were found to be responsible for five DIBs in the spectral region that spans ∼900−970 nm.[48−50] The photoprocessing in this work

https://doi.org/10.1021/jacs.5c08619
J. Am. Chem. Soc. 2025, 147, 34508−34516

underlines the connection between PAHs and fullerenes and suggests that the photoisomerization products of PAHs should also be considered as potential DIB carriers. Future studies focused on recording the optical spectra of the product ions formed by the photodissociation of PAHs are needed to test this hypothesis.

The 30 eV electron gun employed in this study will leave the PAH, after ionization, with an excess internal energy of ∼22 eV minus the kinetic energy carried away by the electron, which can be substantial. In photodissociation regions in the interstellar medium, photon energies are limited to less than the atomic hydrogen ionization energy (13.6 eV) and are typically of the order of 8.1 eV.[51] Hence, absorption of a single far ultraviolet (FUV) photon by an interstellar PAH cation will not leave the species sufficiently excited to promote the isomerization and H and H_2 loss processes studied here. However, photoprocessing of interstellar PAHs is dominated by two-photon processes where a second FUV photon is absorbed before the excitation energy of the first FUV photon is radiated away,[19,34] and such events would leave the PAH sufficiently excited to cross the energy barriers involved in the isomerization and H and H_2 loss processes described here (cf., Figure 6). With a typical FUV photon being absorbed every ≃3000 s and a radiative cooling time scale of 0.1 s, the probability of such an event is rare ($\simeq 3 \times 10^{-5}$).[19,34] Nevertheless, over relevant interstellar dynamical time scales (10^5 yr), some 3×10^4 such events could occur. Likewise, absorption of an X-ray photon by a PAH will leave an internal vibrational excitation of some 20 eV (cf., Reitsma et al.[52] and references therein) and would therefore promote the processes studied here. X-ray processing of PAHs is of prime importance in planet-forming disks around young solar-type stars.[53] In either of these environments—PDRs and planet-forming disks—PAHs play an important role in the energy balance of the gas,[54−57] they are a key component of the organic inventory, and they dominate the mid-infrared spectral energy distribution. Models for such a region will therefore have to take the isomerization and dehydrogenation processes described here into account.

4. EXPERIMENTAL SECTION

The experiments were conducted on the cryogenically cooled 22-pole ion trap instrument, FELion, which was connected to the free electron laser FEL-2 of the FELIX Laboratory at Radboud University, Nijmegen, The Netherlands.[58] The FELion system has been described in detail in prior publications,[59] and here we only focus on the relevant experimental details.

Two isomeric PAH samples, anthracene and phenanthrene ($C_{14}H_{10}$, Sigma-Aldrich, ≥98% and 98% pure, respectively, see Figure 1 for their structures) were evaporated into an electron impact ionization source at pressures of several 10^{-5} mbar. Gas phase PAH species were subsequently ionized by electron ionization using an electron energy of either 30 eV for doubly dehydrogenated species or 40 eV for the singly dehydrogenate ions. Electron ionization at these energies not only yielded the parent radical cation but also resulted in signals that correspond to the loss of one or two hydrogen atoms from the parent cation. The ions were subsequently guided through a quadrupole mass selector, and the daughter ions within a mass range of about 4 amu were admitted to the cryogenically cooled ion trap.

The (doubly) dehydrogenated cations of interest were admitted to the cryogenically cooled trap held at a temperature range of 4−10 K. van der Waals bound clusters of the mass-selected cation of interest and neon were made by exposing the ion cloud to a brief and intense pulse of a helium/neon mixture in a 3:1 ratio. The cluster ions were subsequently exposed to tunable radiation from the infrared free electron laser (FEL-2) at the FELIX Laboratory that provides macropulses with energies up to 120 mJ per pulse (with around 7−30 mJ per pulse in the trap region) at a repetition rate of 10 Hz and with a fwhm bandwidth of $\Delta\nu = = (0.7-1.2)\%\cdot\nu =)$. Each FEL macropulse consists of a train of micropulses separated by 1 ns. The photon energy was tuned between 600 and 1800 cm^{-1} with a step size of 1 cm^{-1}. The ion cloud was exposed to the infrared radiation for (1.6−2.6) s, and the trap contents are then analyzed using a second mass filter coupled to a Daly detector to investigate the degree of dissociation of the cluster ions as a function of frequency. The spectrum was normalized using the following equation

$$I = \frac{-\ln(N_{on}(\nu)/N_{off}(\nu))}{n\cdot P/(h\cdot\nu)}$$

where I is the intensity in units of relative cross-section per photon, P is the laser pulse energy at the trap location, n is the number of pulses, $N_{on}(\nu)$ represents the number of complexed ions at a given frequency ν, and N_{off} is the baseline value. This method has previously been applied to investigate the structures of a number of PAH cation dissociation products.[32,38]

Multiple isomeric products may be formed upon dissociative electron ionization. To disentangle the contributions of such fragment isomers that were potentially produced in the ion source, we performed saturation-depletion scans.[59] For the latter measurements, we exposed the tagged ions to radiation corresponding to the maximum absorption of a specific isolated vibrational band and applied a large number of FELIX macro-pulses. The depletion of the tagged ions at that frequency was compared to the ion signal observed at an off-resonance frequency to account for any losses due to nonradiative processes. The saturation-depletion value directly yielded the relative abundance of the isomer or multiple isomers that were responsible for the selected vibrational normal mode.

5. COMPUTATIONAL METHOD

Isomeric assignments to daughter ions were made by comparing the experimental IR predissociation spectra to the computed spectra. Electronic structure calculations were employed to obtain the energies and harmonic IR spectra of suspect dissociation fragments isomers. All calculations were performed using DFT within the Gaussian16 suite of programs with the B3LYP functional and the 6-311++G(2d,p) basis set.[60−62] This combination has been shown in the past to provide an accurate representation of frequencies for aromatic hydrocarbon compounds and their cations.[38] We employed a scaling factor of 0.983 to account for anharmonicities.[63]

The $C_{14}H_{10}^{\bullet+}$ PES of the dissociation was scanned to provide insights into the formation of our identified product ion isomers. Relaxed scans and QST3 calculations were performed to locate the transition states. Each saddle point was identified by analysis of the imaginary normal mode, and intrinsic reaction coordinate calculations were employed to verify that each transition state connected the appropriate local minima. Optimization and frequency calculations of all intermediates and transition states were performed using the same B3LYP/6-311++G(2d,p) level of theory.

■ ASSOCIATED CONTENT

Supporting Information

The Supporting Information is available free of charge at https://pubs.acs.org/doi/10.1021/jacs.5c08619.

Experimental and calculated IR band positions, comparisons of the measured **ddAnt**$^{\bullet+}$ and **ddPhe**$^{\bullet+}$ spectra with canonical products, saturation-depletion data, and supplemental PES calculations (PDF)

https://doi.org/10.1021/jacs.5c08619
J. Am. Chem. Soc. 2025, 147, 34508−34516

AUTHOR INFORMATION

Corresponding Author

Jordy Bouwman − *Laboratory for Atmospheric and Space Physics, University of Colorado, Boulder, Colorado 80303, United States; Department of Chemistry, University of Colorado, Boulder, Colorado 80309, United States; Institute for Modeling Plasma, Atmospheres and Cosmic Dust (IMPACT), NASA/SSERVI, Boulder, Colorado 80309, United States;* orcid.org/0000-0002-3615-1703; Email: jordy.bouwman@colorado.edu

Authors

Madison M. Patch − *Laboratory for Atmospheric and Space Physics, University of Colorado, Boulder, Colorado 80303, United States; Department of Chemistry, University of Colorado, Boulder, Colorado 80309, United States; Institute for Modeling Plasma, Atmospheres and Cosmic Dust (IMPACT), NASA/SSERVI, Boulder, Colorado 80309, United States*

Rory McClish − *Laboratory for Atmospheric and Space Physics, University of Colorado, Boulder, Colorado 80303, United States; Department of Chemistry, University of Colorado, Boulder, Colorado 80309, United States; Institute for Modeling Plasma, Atmospheres and Cosmic Dust (IMPACT), NASA/SSERVI, Boulder, Colorado 80309, United States*

Sanjana Panchagnula − *Laboratory for Astrophysics, Leiden Observatory, Leiden University, 2300 RA Leiden, The Netherlands*

Daniël B. Rap − *HFML-FELIX, 6525 ED Nijmegen, The Netherlands; Institute for Molecules and Materials, Radboud University, 6525 AJ Nijmegen, The Netherlands*

Shreyak Banhatti − *HFML-FELIX, 6525 ED Nijmegen, The Netherlands; Institute for Molecules and Materials, Radboud University, 6525 AJ Nijmegen, The Netherlands; I. Physikalisches Institut, Universität zu Köln, 50937 Köln, Germany*

Helgi R. Hrodmarsson − *Université Paris Est Créteil and Université Paris Cité, CNRS, LISA UMR 7583, 94010 Créteil, France*

Sandra Brünken − *HFML-FELIX, 6525 ED Nijmegen, The Netherlands; Institute for Molecules and Materials, Radboud University, 6525 AJ Nijmegen, The Netherlands;* orcid.org/0000-0001-7175-4828

Harold Linnartz − *Laboratory for Astrophysics, Leiden Observatory, Leiden University, 2300 RA Leiden, The Netherlands;* orcid.org/0000-0002-8322-3538

Alexander G. G. M. Tielens − *Department of Astronomy, University of Maryland, College Park, Maryland 20742-2421, United States; Leiden Observatory, Leiden University, 2300 RA Leiden, The Netherlands*

Complete contact information is available at: https://pubs.acs.org/10.1021/jacs.5c08619

Notes

The authors declare no competing financial interest.

ACKNOWLEDGMENTS

This work was supported in part by NASA's Solar System Exploration Research Virtual Institute (SSERVI): Institute for Modeling Plasma, Atmosphere, and Cosmic Dust (IMPACT). This material is based on the work supported by the National Science Foundation under Grant No. 2308045. This work utilized the Alpine high-performance computing resource at the University of Colorado Boulder. Alpine is jointly funded by the University of Colorado Boulder, the University of Colorado Anschutz, and Colorado State University. We gratefully acknowledge the support of the Radboud University and of the Nederlandse Organisatie voor Wetenschappelijk Onderzoek (NWO) for providing the required beam time at the FELIX laboratory and the skillful assistance of the FELIX staff. S.Ba. and S.P. acknowledge funding through the Marie Skłodowska Curie Actions (MSCA) Innovative Training Networks (ITN) H2020-MSCA-ITN 2016 (EUROPAH project, G. A. 722346). H.R.H. acknowledges funding from the European Union's Horizon 2020 research and innovation programme under grant agreement No. 838372. We thank the Cologne Laboratory Astrophysics group for providing the FELion ion trap instrument for the current experiments and the Cologne Center for Terahertz Spectroscopy funded by the Deutsche Forschungsgemeinschaft (DFG, grant SCHL 341/15-1) for supporting its operation.

REFERENCES

(1) Peeters, E.; Spoon, H. W. W.; Tielens, A. G. G. M. Polycyclic aromatic hydrocarbons as a tracer of star formation? *Astrophys. J.* **2004**, *613*, 986−1003.

(2) Tielens, A. G. G. M. Interstellar polycyclic aromatic hydrocarbons. *Annu. Rev. Astron. Astrophys.* **2008**, *46*, 289−337.

(3) Hrodmarsson, H. R.; Aleman, I.; Candian, A.; Wiersma, S.; Palotás, J.; Dubois, D.; Sidhu, A.; Loru, D.; Sundarajan, P.; Sciamma-O'Brien, E.; Tielens, A. G. G. M. The AstroPAH 10 Years of Science Review. *Space Sci. Rev.* **2025**, *221*, 42.

(4) Leger, A.; Puget, J. L. Identification of the unidentified infrared emission features of interstellar dust. *Astron. Astrophys.* **1984**, *137*, L5−L8.

(5) Allamandola, L. J.; Tielens, A. G. G. M.; Barker, J. R. Polycyclic aromatic hydrocarbons and the unidentified infrared emission bands: auto exhaust along the milky way. *Astrophys. J., Lett.* **1985**, *290*, L25−L28.

(6) Allamandola, L. J.; Tielens, A. G. G. M.; Barker, J. Interstellar polycyclic aromatic hydrocarbons: The infrared emission bands, the excitation/emission mechanism, and the astrophysical implications. *Astrophys. J., Suppl. Ser.* **1989**, *71*, 733−775.

(7) Cernicharo, J.; Agúndez, M.; Kaiser, R. I.; Cabezas, C.; Tercero, B.; Marcelino, N.; Pardo, J. R.; de Vicente, P. Discovery of benzyne, o-C_6H_4, in TMC-1 with the QUIJOTE line survey. *Astron. Astrophys.* **2021**, *652*, L9.

(8) McGuire, B. A.; Loomis, R. A.; Burkhardt, A. M.; Lee, K. L. K.; Shingledecker, C. N.; Charnley, S. B.; Cooke, I. R.; Cordiner, M. A.; Herbst, E.; Kalenskii, S.; Siebert, M. A.; Willis, E. R.; Xue, C.; Remijan, A. J.; McCarthy, M. C. Detection of two interstellar polycyclic aromatic hydrocarbons via spectral matched filtering. *Science* **2021**, *371*, 1265−1269.

(9) Wenzel, G.; et al. Detection of interstellar 1-cyanopyrene: A four-ring polycyclic aromatic hydrocarbon. *Science* **2024**, *386*, 810−813.

(10) Wenzel, G.; et al. Detections of interstellar aromatic nitriles 2-cyanopyrene and 4-cyanopyrene in TMC-1. *Nat. Astron.* **2025**, *9*, 262−270.

(11) Tielens, A. G. G. M. The molecular universe. *Rev. Mod. Phys.* **2013**, *85*, 1021−1081.

(12) Ryan, C.; et al. PDRs4All—IV. An embarrassment of riches: Aromatic infrared bands in the Orion Bar. *Astron. Astrophys.* **2024**, *685*, A75.

(13) Andrews, H.; Boersma, C.; Werner, M. W.; Livingston, J.; Allamandola, L. J.; Tielens, A. G. G. M. PAH Emission at the Bright Locations of PDRs: the grandPAH Hypothesis. *Astrophys. J.* **2015**, *807*, 99.

(14) Bauschlicher, J.; Charles, W.; Peeters, E.; Allamandola, L. J. The Infrared Spectra of Very Large, Compact, Highly Symmetric, Polycyclic Aromatic Hydrocarbons (PAHs). *Astrophys. J.* **2008**, *678*, 316−327.
(15) Bauschlicher, C. W.; Peeters, E.; Allamandola, L. J.; Allamandola, L. J. The Infrared Spectra of Very Large Irregular Polycyclic Aromatic Hydrocarbons (PAHs): Observational Probes of Astronomical PAH Geometry, Size, and Charge. *Astrophys. J.* **2009**, *697*, 311−327.
(16) Ricca, A.; Bauschlicher, C. W.; Boersma, C.; Tielens, A. G. G. M.; Allamandola, L. J.; Allamandola, L. J. The Infrared Spectroscopy of Compact Polycyclic Aromatic Hydrocarbons Containing up to 384 Carbons. *Astrophys. J.* **2012**, *754*, 75.
(17) Stein, S. On the High Temperature Chemical Equilibria of Polycyclic Aromatic Hydrocarbons. *J. Phys. Chem.* **1978**, *82*, 566−571.
(18) Murga, M. S.; Kirsanova, M. S.; Vasyunin, A. I.; Pavlyuchenkov, Y. N. Impact of PAH photodissociation on the formation of small hydrocarbons in the Orion Bar and the horsehead PDRs. *MNRAS* **2020**, *497*, 2327−2339.
(19) Berné, O.; Montillaud, J.; Joblin, C. Top-down formation of fullerenes in the interstellar medium. *Astron. Astrophys.* **2015**, *577*, A133.
(20) Berné, O.; Tielens, A. G. G. M. Formation of buckminsterfullerene (C_{60}) in interstellar space. *Proc. Natl. Acad. Sci. U.S.A.* **2012**, *109*, 401−406.
(21) West, B. J.; Lesniak, L.; Mayer, P. M. Why Do Large Ionized Polycyclic Aromatic Hydrocarbons Not Lose C_2H_2? *J. Phys. Chem. A* **2019**, *123*, 3569−3574.
(22) Zhen, J.; Paardekooper, D. M.; Candian, A.; Linnartz, H.; Tielens, A. G. G. M. Quadrupole ion trap/time-of-flight photofragmentation spectrometry of the hexa-*peri*-hexabenzocoronene (HBC) cation. *Chem. Phys. Lett.* **2014**, *592*, 211−216.
(23) Zhen, J.; Castellanos, P.; Paardekooper, D. M.; Linnartz, H.; Tielens, A. G. G. M. Laboratory formation of fullerenes from PAHs - top-down interstellar chemistry. *Astrophys. J., Lett.* **2014**, *797*, L30.
(24) Bouwman, J.; Sztáray, B.; Oomens, J.; Hemberger, P.; Bodi, A. Dissociative Photoionization of Quinoline and Isoquinoline. *J. Phys. Chem. A* **2015**, *119*, 1127−1136.
(25) West, B.; Useli-Bacchitta, F.; Sabbah, H.; Blanchet, V.; Bodi, A.; Mayer, P. M.; Joblin, C. Photodissociation of Pyrene Cations: Structure and Energetics from $C_6H^+_{10}$ to C^+_{14} and Almost Everything in Between. *J. Phys. Chem. A* **2014**, *118*, 7824−7831.
(26) Hrodmarsson, H. R.; Bouwman, J.; Tielens, A. G. G. M.; Linnartz, H. Similarities and dissimilarities in the fragmentation of polycyclic aromatic hydrocarbon cations: A case study involving three dibenzopyrene isomers. *Int. J. Mass Spectrom.* **2022**, *476*, 116834.
(27) Rap, D. B.; van Boxtel, T. J. H. H.; Redlich, B.; Brünken, S. Spectroscopic Detection of Cyano-Cyclopentadiene Ions as Dissociation Products upon Ionization of Aniline. *J. Phys. Chem. A* **2022**, *126*, 2989−2997.
(28) Hrodmarsson, H. R.; Bouwman, J.; Tielens, A. G.; Linnartz, H. Fragmentation of the PAH cations of Isoviolanthrene and Dicoronylene: A case made for interstellar cyclo[n]carbons as products of universal fragmentation processes. *Int. J. Mass Spectrom.* **2023**, *485*, 116996.
(29) Schleier, D.; Kamer, J.; Jiao, A.; Schneider, G. F.; Linnartz, H.; Bouwman, J. Photoprocessing of cationic triazacoronene: dissociation characteristics of polycyclic aromatic nitrogen heterocycles in interstellar environments. *Phys. Chem. Chem. Phys.* **2024**, *26*, 15547−15558.
(30) Panchagnula, S.; Kamer, J.; Candian, A.; Hrodmarsson, H. R.; Linnartz, H.; Bouwman, J.; Tielens, A. G. G. M. Laser-induced fragmentation of coronene cations. *Phys. Chem. Chem. Phys.* **2024**, *26*, 18557−18570.
(31) de Haas, A. J.; Oomens, J.; Bouwman, J. Facile pentagon formation in the dissociation of polyaromatics. *Phys. Chem. Chem. Phys.* **2017**, *19*, 2974−2980.
(32) Banhatti, S.; Rap, D. B.; Simon, A.; Leboucher, H.; Wenzel, G.; Joblin, C.; Redlich, B.; Schlemmer, S.; Brünken, S. Formation of the acenaphthylene cation as a common C_2H_2-loss fragment in dissociative ionization of the PAH isomers anthracene and phenanthrene. *Phys. Chem. Chem. Phys.* **2022**, *24*, 27343−27354.
(33) Wakelam, V.; Bron, E.; Cazaux, S.; Dulieu, F.; Gry, C.; Guillard, P.; Habart, E.; Hornekær, L.; Morisset, S.; Nyman, G.; Pirronello, V.; Price, S. D.; Valdivia, V.; Vidali, G.; Watanabe, N. H_2 formation on interstellar dust grains: The viewpoints of theory, experiments, models and observations. *Molecular Astrophysics* **2017**, *9*, 1−36.
(34) Andrews, H.; Candian, A.; Tielens, A. G. G. M. Hydrogenation and dehydrogenation of interstellar PAHs: Spectral characteristics and H_2 formation. *Astron. Astrophys.* **2016**, *595*, A23.
(35) Castellanos, P.; Candian, A.; Andrews, H.; Tielens, A. G. G. M. Photoinduced polycyclic aromatic hydrocarbon dehydrogenation. Molecular hydrogen formation in dense PDRs. *Astron. Astrophys.* **2018**, *616*, A167.
(36) Alvaro-Galué, H.; Oomens, J. Spectroscopic Evidence for a Triplet Ground State in the Naphthyl Cation. *Angew. Chem., Int. Ed.* **2011**, *50*, 7004−7007.
(37) Alvaro Galué, H.; Oomens, J. On the Electronic Structure of Isolated Mono-dehydrogenated Polyaromatic Hydrocarbon Ions and Their Astrophysical Relevance. *Astrophys. J.* **2012**, *746*, 83.
(38) Panchagnula, S.; Bouwman, J.; Rap, D. B.; Castellanos, P.; Candian, A.; Mackie, C.; Banhatti, S.; Brünken, S.; Linnartz, H.; Tielens, A. G. G. M. Structural investigation of doubly-dehydrogenated pyrene cations. *Phys. Chem. Chem. Phys.* **2020**, *22*, 21651−21663.
(39) Simon, A.; Rapacioli, M.; Rouaut, G.; Trinquier, G.; Gadéa, F. X. Dissociation of polycyclic aromatic hydrocarbons: molecular dynamics studies. *Philos. Trans. R. Soc., A* **2017**, *375*, 20160195.
(40) Hager, J. W.; Wallace, S. C. Two-laser photoionization supersonic jet mass spectrometry of aromatic molecules. *Anal. Chem.* **1988**, *60*, 5−10.
(41) Kroto, H. W.; Heath, J. R.; O'Brien, S. C.; Curl, R. F.; Smalley, R. E. C_{60}: Buckminsterfullerene. *Nature* **1985**, *318*, 162−163.
(42) Kroto, H. W. The stability of the fullerenes C_n, with n = 24, 28, 32, 36, 50, 60 and 70. *Nature* **1987**, *329*, 529−531.
(43) Aihara, J.-i. Bond Resonance Energy and Verification of the Isolated Pentagon Rule. *J. Am. Chem. Soc.* **1995**, *117*, 4130−4136.
(44) Wakabayashi, T.; Shiromaru, H.; Kikuchi, K.; Achiba, Y. A. selective isomer growth of fullerenes. *Chem. Phys. Lett.* **1993**, *201*, 470−474.
(45) Yamaguchi, Y.; Maruyama, S. A molecular dynamics simulation of the fullerene formation process. *Chem. Phys. Lett.* **1998**, *286*, 336−342.
(46) Boersma, C.; Bauschlicher, C. W.; Ricca, A.; Mattioda, A. L.; Cami, J.; Peeters, E.; de Armas, F. S.; Saborido, G. P.; Hudgins, D. M.; Allamandola, L. J. The NASA Ames PAH IR Spectroscopic Database Version 2.00: Updated Content, Web Site and On(Off)line Tools. *Astrophys. J., Suppl. Ser.* **2014**, *211*, 8.
(47) Heger, M. L. The spectra of certain class B stars in the regions 5630A-6680A and 3280A-3380A. *Lick Obs. Bull.* **1922**, *10*, 146−147.
(48) Campbell, E. K.; Holz, M.; Gerlich, D.; Maier, J. P. Laboratory confirmation of C_{60}^+ as the carrier of two diffuse interstellar bands. *Nature* **2015**, *523*, 322−323.
(49) Spieler, S.; Kuhn, M.; Postler, J.; Simpson, M.; Wester, R.; Scheier, P.; Ubachs, W.; Bacalla, X.; Bouwman, J.; Linnartz, H. C_{60}^+ and the Diffuse Interstellar Bands: An Independent Laboratory Check. *Astrophys. J.* **2017**, *846*, 168.
(50) Linnartz, H.; Cami, J.; Cordiner, M.; Cox, N.; Ehrenfreund, P.; Foing, B.; Gatchell, M.; Scheier, P. C_{60}^+ as a diffuse interstellar band carrier; a spectroscopic story in 6 acts. *J. Mol. Spectrosc.* **2020**, *367*, 111243.
(51) Knight, C.; Peeters, E.; Stock, D. J.; Vacca, W. D.; Tielens, A. G. G. M. Tracing PAH Size in Prominent Nearby Mid-Infrared Environments. *Astrophys. J.* **2021**, *918*, 8.
(52) Reitsma, G.; Boschman, L.; Deuzeman, M. J.; Hoekstra, S.; Hoekstra, R.; Schlathölter, T. Near edge X-ray absorption mass spectrometry on coronene. *J. Chem. Phys.* **2015**, *142*, 024308.

https://doi.org/10.1021/jacs.5c08619
J. Am. Chem. Soc. 2025, 147, 34508−34516

(53) Lange, K. Hidden in the dark: Seeking the vanished polycylic aromatic hydrocarbons in planet-forming discs. Ph.D. thesis, University of Amsterdam, 2024.
(54) Verstraete, L.; Leger, A.; D'Hendecourt, L.; Defourneau, D.; Dutuit, O. Ionization cross-section measurements for two PAH molecules - Implications for the heating of diffuse interstellar gas. *Astron. Astrophys.* **1990**, *237*, 436−444.
(55) Bakes, E. L. O.; Tielens, A. G. G. M. The Photoelectric Heating Mechanism for Very Small Graphitic Grains and Polycyclic Aromatic Hydrocarbons. *Astrophys. J., Lett.* **1994**, *427*, 822.
(56) Woitke, P.; Kamp, I.; Thi, W. F. Radiation thermo-chemical models of protoplanetary disks. I. Hydrostatic disk structure and inner rim. *Astron. Astrophys.* **2009**, *501*, 383−406.
(57) Hrodmarsson, H. R.; Verstraete, L.; Dartois, E.; Fréreux, J.; Lacinbala, O.; Nahon, L.; Garcia, G. A.; Pino, T.; Bréchignac, P. Photoionization of small neutral polycyclic aromatic hydrocarbons: Testing photoelectric models of interstellar dust. *Astron. Astrophys.* **2025**, *698*, A202.
(58) Oepts, D.; van der Meer, A.; van Amersfoort, P. The Free-Electron-Laser user facility FELIX. *Infrared Phys. Technol.* **1995**, *36*, 297−308.
(59) Jusko, P.; Brünken, S.; Asvany, O.; Thorwirth, S.; Stoffels, A.; van der Meer, L.; Berden, G.; Redlich, B.; Oomens, J.; Schlemmer, S. The FELion cryogenic ion trap beam line at the FELIX free-electron laser laboratory: infrared signatures of primary alcohol cations. *Faraday Discuss.* **2019**, *217*, 172−202.
(60) Frisch, M. J.; et al. *Gaussian 16*. Revision C.01.; Gaussian Inc: Wallingford CT, 2016.
(61) McLean, A. D.; Chandler, G. S. Contracted Gaussian basis sets for molecular calculations. I. Second row atoms, Z = 11−18. *J. Chem. Phys.* **1980**, *72*, 5639−5648.
(62) Clark, T.; Chandrasekhar, J.; Spitznagel, G. W.; Schleyer, P. V. R. Efficient diffuse function-augmented basis sets for anion calculations. III. The 3−21+G basis set for first-row elements, Li−F. *J. Comput. Chem.* **1983**, *4*, 294−301.
(63) Andersson, M. P.; Uvdal, P. New Scale Factors for Harmonic Vibrational Frequencies Using the B3LYP Density Functional Method with the Triple-ζ Basis Set 6−311+G(d,p). *J. Phys. Chem. A* **2005**, *109*, 2937−2941.

https://doi.org/10.1021/jacs.5c08619
J. Am. Chem. Soc. 2025, 147, 34508−34516